Understanding TES microcalorimeter noise and energy resolution ☆

Wouter Bergmann Tiest*, Marcel Bruijn, Henk Hoevers, Piet de Korte,
Jan van der Kuur, Wim Mels

SRON National Institute for Space Research, Sorbonnelaan 2, Utrecht 3584 CA, The Netherlands

Abstract

We have performed numerical calculations of the noise in voltage-biased superconducting transition edge-based X-ray microcalorimeters, using a finite-element model. Details of the model are discussed, as well as results for different absorber geometries. The results are in agreement with an analytical model and show that the amount of internal thermal fluctuation noise can be reduced by using a segmented absorber. The simulation also agrees well with experimental data, which, for our detectors, contain no major unidentified noise sources. Furthermore, the discrepancy between the (small-signal) theoretical and the measured energy resolutions for 5.9 keV X-rays, for our sensors typically a factor of ~ 2, is explained by a more accurate modelling of the sensor responsivity, taking into account the large signal behaviour.

© 2003 Elsevier B.V. All rights reserved.

1. Introduction

SRON develops microcalorimeters for high-resolution soft X-ray spectroscopy (1–10 keV). These devices consist of a Cu/Bi absorber on top of a Ti/Au transition edge thermometer (TES). They are operated at low temperature under voltage bias [1] and read out using a SQUID amplifier. The small-signal responsivity of the system as a function of frequency is given by

$$S(f) = \frac{V\alpha}{GT(R + R_s)} \frac{1}{1 + \beta L_0} \frac{1}{\sqrt{1 + 4\pi^2 \tau_{\text{eff}}^2 f^2}} \quad (1)$$

with V the voltage over the TES, $\alpha \equiv (T/R)(\mathrm{d}R/\mathrm{d}T)$, G the dynamic thermal conductance to the bath, T the TES temperature, R the TES resistance, R_s the shunt resistance, $\beta \equiv (R - R_s)/(R + R_s)$, $L_0 \equiv V^2\alpha/(RGT)$, $\tau_{\text{eff}} \equiv C/G/(1 + \beta L_0)$ and C the heat capacity. The noise at the output is mainly composed of phonon noise due to thermal fluctuations over the link to the bath, Johnson noise from the TES resistance and internal thermal fluctuation noise (ITFN) from the fluctuations over the thermal conductance of the TES itself [2]. By dividing this by $S(f)$, the noise equivalent power (NEP) is found. If optimum filtering is used, the theoretical FWHM energy resolution can be calculated from the NEP [3] and is given by

$$\Delta E = 2.36\xi\sqrt{k_B T^2 C} \quad (2)$$

with

$$\xi = 2\sqrt[4]{\gamma\left(\frac{1}{\alpha L_0} + \frac{G}{G_{\mathrm{TES}}}\right) + \left(\frac{1}{\alpha L_0} + \frac{G}{G_{\mathrm{TES}}}\right)^2} \qquad (3)$$

where $\gamma \approx 0.5$ is a parameter describing the thermal gradient over the heat link to the bath and G_{TES} is the internal thermal conductance of the TES. In the following sections the dependence of the ITFN on the device geometry and the validity of the small-signal responsivity model are examined.

2. ITFN and geometry

ITFN is the result of thermal fluctuations present in the TES itself. The presence of this noise component in our devices has been demonstrated in Refs. [2,4]. We have investigated the ITFN by numerically modelling the device as an array of elements connected to each other by electrical and thermal links. Across these links, noise sources were applied. Thus, a current noise spectrum could be calculated.

In a homogeneous device, with all elements identical, the ITFN is only visible as a second-order effect and of no significance for the current noise spectrum. A movement of heat from one location to another causes a temperature drop in the first location and a temperature rise of equal magnitude in the second. Since the temperature sensitivity is identical too, the ensuing resistance changes will also be equal and opposite. Therefore, in first order there will be no net effect on the current through the device.

In a configuration with a central absorber surrounded by a TES, the ITFN is much more visible. The absorber has a different heat capacity and temperature sensitivity than the TES. Therefore, heat fluctuations occurring across the boundary between absorber and TES have a visible effect on the current through the device. The simulation shows that the ITFN in a device with a central absorber is very similar to the ITFN in a lateral TES/absorber configuration, where the current

noise spectrum can be described by

$$i_{\mathrm{ITFN}}(f) = \frac{\delta T_{\mathrm{n}} V \alpha}{T(R + R_{\mathrm{s}})} \frac{1}{1 + \beta L_0}$$
$$\times \sqrt{\frac{1 + 4\pi^2\tau^2 f^2}{1 + 4\pi^2\tau_{\mathrm{eff}}^2 f^2}} \frac{1}{\sqrt{1 + f^2/f_{\mathrm{TES}}^2}} \qquad (4)$$

with δT_{n} the magnitude of the visible thermal fluctuations in the TES (in $\mathrm{K}/\sqrt{\mathrm{Hz}}$), $\tau \equiv C/G$ and f_{TES} the cut-off frequency of the thermal fluctuations. This noise component introduces a "bump" in the spectrum at higher frequencies.

In order to manipulate this noise component, we modelled sensors with a number of normal metal sections extending over the full-width of the TES, perpendicular to the direction of the current. The width of the absorber stripes is the same as the width of the TES parts in between, and there is a TES part on either end, thus creating $2n + 1$ areas for n stripes. We simulated designs with 1, 2, 3, 4 and 13 stripes while keeping the total heat capacity and internal thermal conductivity constant. The noise curves were fitted to obtain a value for the parameter δT_{n} (Fig. 1). The dependence on the number of stripes can be understood as follows. Consider a 1-dimensional TES with a heat capacity C_{TES} and an internal thermal conductivity G_{TES}. On top of the TES are n absorber stripes, suppressing the temperature sensitivity of the TES in those places. The absorber stripes form local heat baths, with a TES piece the width of half a stripe on either side. This TES piece has a heat
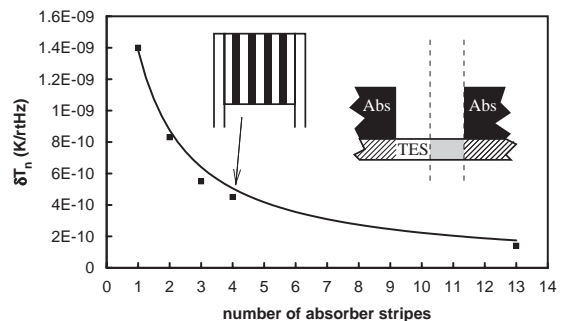

Fig. 1. Value of the ITFN parameter δT_{n} as a function of the number of absorber stripes. The squares are the results of the numerical simulation while the curve is an analytical expression. The inset shows a section view of the device with a single TES piece shaded.

capacity $C_1 = C_{TES}/(4n+2)$ and a thermal conductance $G_1 = (4n+2)G_{TES}$. Therefore, the cut-off frequency of the thermal fluctuations in one element is

$$f_1 = \frac{G_1}{2\pi C_1} = (4n+2)^2 \frac{G_{TES}}{2\pi C_{TES}}. \qquad (5)$$

Since all elements are identical, the spectrum of the whole TES has the same cut-off frequency as a single element. It has the form

$$\langle \Delta T^2(f) \rangle = \delta T_n^2 \frac{1}{1 + f^2/f_1^2}. \qquad (6)$$

Integrated over all frequencies, this quantity should be normalised to the total amount of thermal fluctuations in all TES pieces not covered by an absorber, which is $(2n+1)k_B T^2/(n+1)C_{TES}$. Solving for δT_n, we get

$$\delta T_n = \sqrt{\frac{1}{(n+1)(2n+1)} \frac{k_B T^2}{G_{TES}}}. \qquad (7)$$

This theoretical relation is also plotted in Fig. 1 and agrees well with the simulation results.

The effect of reduction of the ITFN level has also been demonstrated experimentally. In Fig. 2, the current noise spectrum of a 4-stripe sensor is plotted. Only a small ITFN component is present and the spectrum is dominated by phonon and Johnson noise. This reduction in noise level compared to a device with a central absorber
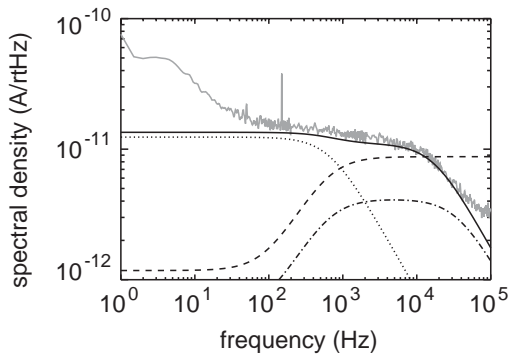
should improve the energy resolution. However, the bars introduce an extra resistance in the circuit, which resulted in a lower value for the effective α which has a negative effect on the energy resolution. A 2-D simulation has shown that a design with the stripes not extending all the way to the edge of the TES has a similar low ITFN component without the drawback of the series resistance.

3. Responsivity model

Despite our good understanding of the noise in our devices, the calculated expected energy resolution using Eqs. (2) and (3) is generally a factor ~ 2 better than the measured resolution at 5.9 keV. We attribute this to a substantial deviation of the responsivity from the small-signal model, Eq. (1). In Fig. 3, the normalised responsivity is plotted based on the small-signal analytical model and on a large-signal numerical model. Our filtering consists of convolving the measured signal with the pulse shape (responsivity). It is clear that in the small-signal model less noise passes through the filter and so it results in a smaller resolution figure. We have used the real measured pulse shape and measured noise spectrum to calculate the expected resolution (Table 1). Using this formalism, the agreement between measured and calculated resolution is generally better than 1 eV ($<20\%$).

Fig. 2. Measured current noise spectrum of the device "X047" with a 4-stripe absorber (grey). The low-frequency component is a measurement artefact and does not originate from the sensor. Also plotted are theoretical curves for phonon noise (dotted), Johnson noise (dashed), ITFN (dash–dotted) and total theoretical noise (solid).
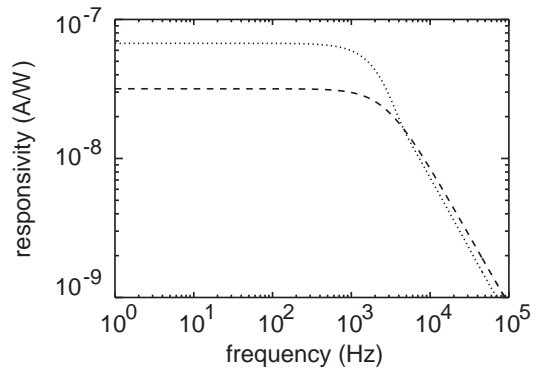

Fig. 3. Responsivity curves for the small-signal (dashed) and large-signal (dotted) models, normalised to equal filtered-signal output.

Table 1
Measured and calculated energy resolutions at 5.9 keV for different devices

Device	Measured (eV)	Calculated (eV)	
		SS	LS
X037	4.2	2.1	4.4
X038	4.1	1.5	4.3
X043	4.7	3.0	3.9
X047	15.7	1.9	15.8
X049	5.3	2.4	4.7
X055-6	4.5	1.3	3.3

SS is small-signal using Eqs. (2)–(3); LS is large-signal using the measured pulse shape and noise spectrum.

We conclude that because the pulse shape (responsivity) deviates strongly from the exponential shape derived from small-signal theory, the theoretical limit given by Eq. (2) is an under-estimate of the obtainable resolution. A more correct responsivity model can be obtained by a (large-signal) numerical simulation of the device behaviour. Improvement upon the present resolution should be possible by reducing the dominant noise component of ITFN by means of an optimised geometry.

References

[1] K. Irwin, Appl. Phys. Lett. 66 (1995) 1998.
[2] H. Hoevers, A. Bento, M. Bruijn, L. Gottardi, M. Korevaar, W. Mels, P. de Korte, Appl. Phys. Lett. 77 (2000) 4422.
[3] S. Moseley, J. Mather, D. McCammon, J. Appl. Phys. 56 (1984) 1257.
[4] W. Bergmann Tiest, H. Hoevers, W. Mels, M. Ridder, M. Bruijn, P. de Korte, M. Huber, AIP Conf. Proc. 605 (2002) 199.